

A Dual Battery Power Management System for Solar Charging to Improve Charging Efficiency

Peng Yuxi, Zhang Teng*, Zhu Kai, Kong Weifeng, Fu Siwei, Du Xuewu

*School of Mechanical Engineering, Jiangsu University, 212013, Zhenjiang, China
Email:390151059@qq.com

ABSTRACT. *At present, the solar energy used in the Internet of things for agriculture has the characteristics of finiteness, randomness and discontinuity. How to store energy more efficiently in the time of energy storage has become an important problem. In this paper, the polarization of lithium iron phosphate battery is studied, and its constant current constant voltage charging mode is analyzed. A dual power management system is designed by controlling the time of constant voltage charging stage. Compared with the existing scheme, the charging scheme of the system reduces the influence from the battery polarization and improves the charging efficiency.*

KEYWORDS: *Matlab / Simulink, battery management, photovoltaic, power generation, battery polarization Agricultural Internet of things*

1. Introduction

Chinese agriculture is in a period of transition from traditional agriculture to modern agriculture, the Internet of Things industry is emerging, and it is deeply integrated with agriculture^[1]. As an electronic information facility, due to the special situation of wide distribution of application areas, difficulty in power connection, and unstable voltage in the agricultural Internet of Things, the agricultural application scene has sufficient characteristics. More and more Internet of Things devices use solar panels and Battery energy storage as an energy source.^[2]

At present, the charging logic of most photovoltaic charging is the same as that of commercial power charging. The solar energy has the characteristics of finiteness, randomness and discontinuity and the randomness of load demand, which is different from the situation of commercial power. Therefore, the traditional charging method is obviously not suitable. The main factor affecting battery energy storage efficiency is battery polarization. Therefore, by analyzing farmland application

scenarios and exploring the impact of battery polarization on charging efficiency, a set of dual-battery power management mechanisms that improve charging efficiency by controlling the charging time during the constant-voltage charging phase are designed. And by comparing with the conventional charging method, the superiority of the scheme is obtained.

2. Dual Battery Power Design

2.1 Use scenarios and overall system framework

The dual battery power management system is used by connecting two identical batteries and a solar charging module, and the electric energy enters the load through the management system.

The working logic of the dual battery power management system is shown in Figure 1. The battery status judgment module will record the voltage status of the battery (undervoltage, normal, overvoltage). And the logic gate circuit records the state to respond, and transmits the corresponding action to the relevant power consumption judgment module and charging judgment module. The power consumption module and the charging module are independent of each other and do not affect each other. The power judgment module can play the role of battery over-discharge protection and power switching, and it will perform battery switching according to the signal: if the battery in use has an under-voltage condition, it will switch; if both batteries are in the under-voltage state, Stop using electricity. The charging judgment module can play the role of overshoot protection and control the charging time under constant voltage. It will perform battery switching according to the model: if the rechargeable battery reaches a constant current-constant voltage switching voltage, it will start timing to a predetermined time for switching. Both batteries reach a constant voltage and stop charging.

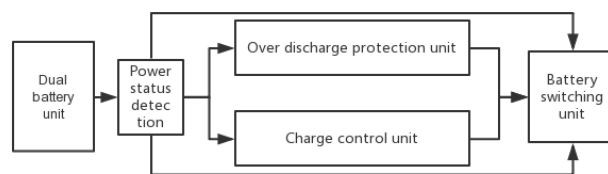


Figure 1: Function

2.2 Realization of battery recording status module

The battery recording status is composed of LM393 voltage comparator, 74HC154 decoder and XL6009 boost module. The two XL6009's voltage is set to the battery's over-discharge voltage and constant voltage charging voltage through the potentiometer. The negative voltage input terminal of the LM393 is connected to the positive input terminal. When the battery voltage is lower than the comparison voltage, the LM393 will be set. 1. The output of the two LM393 can indicate that the battery is in the state 11 is over-discharge, 01 is normal, and 00 is the constant voltage charging set voltage. In this way, the state of the two batteries can be represented by a 4-digit binary number.

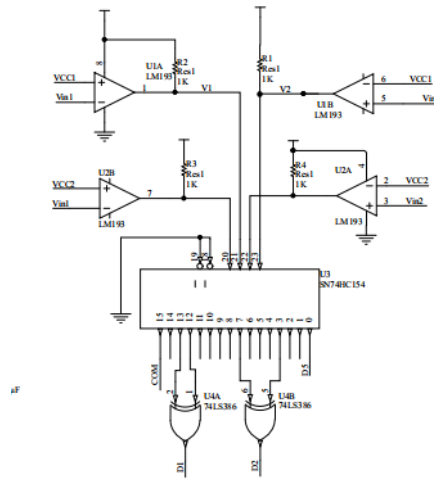


Figure 2: Battery recording status module

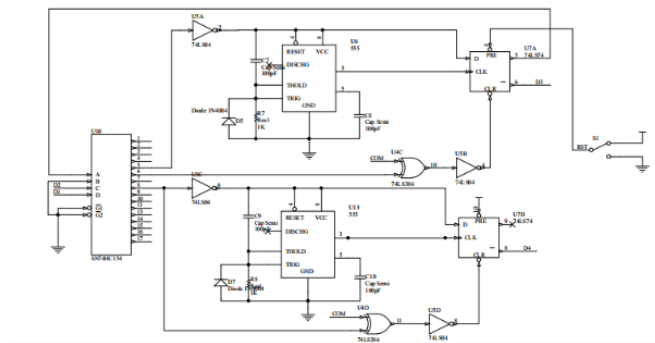


Figure 3: Over-discharge protection and power switching module

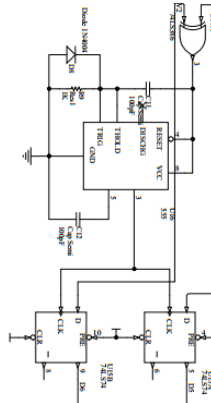


Figure 4: Overshoot protection and charging delay switching module

2.3 Realization of over-discharge protection and power switch

The over-discharge protection circuit is shown in Figure 3, which is composed of 74LS386, 555 timer and its peripheral circuits, 74HC154 decoder, 74LS74 double D flip-flop, 74LS04. Among them, Q1 and Q2 of 74LS74 output signals to judge whether the working state of the connected relay is working. The 74LS386 processes the signal obtained from the battery recording status module to determine whether battery 1 is undervoltage and battery 2 is undervoltage. In this way, the battery status is treated as 4-digit binary information. If the battery needs to be switched in the under-voltage state, change the trigger state, change the connected relay, and use another battery to supply power. If both batteries are under voltage, the transistor is controlled to interrupt the power circuit to prevent overdischarge.

2.4 Realization of overshoot protection and charging delay switching

The over-discharge protection circuit is shown in Figure 4, which is composed of 74LS386, 555 timer and its peripheral circuits, 74LS74 double D flip-flop, 74LS04. The 74LS386 processes the signal obtained from the battery recording status module as to whether the battery 1 voltage has reached the set condition and whether the battery 2 voltage has reached the set condition. If the voltage of the rechargeable battery is at the voltage set in the constant voltage charging stage, the 555 timer starts to count, when the set time is reached, the connected relay is changed, and another battery is charged to achieve the purpose of changing the charging time in the constant voltage stage. If both batteries are in the set state, the transistor is controlled to interrupt the charging circuit to prevent overcharging.

3. Experimental Verification

3.1 Environment construction

APM18M5W27x27 is a commonly used solar panel, this component is used in this study. The peak power of the component is 5W, the peak voltage is 5.75V, and the peak current is 0.57A. The charging method uses the most common constant voltage-constant current charging method. The constant current-constant voltage charging mode has high charging efficiency and less damage to the battery. It is the most commonly used charging method for lithium batteries. Most of the application scenarios that use solar energy storage also use this method to store electricity. According to the above conditions, we establish the following Table 1 as the ideal environment information established according to the preset conditions.

Table 1: Experimental environment information under ideal conditions

Sunshine time	Temperature	Constant voltage	Constant current
160000s	25°C	3.4v	0.5A

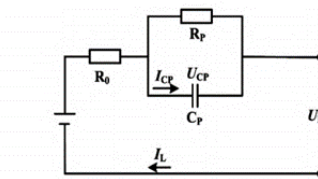


Figure 5: Battery equivalent model

3.2 Establishment of battery model

The design scheme in this paper can effectively avoid the influence of battery polarization on the charging efficiency under the same charging situation. Therefore, it is very important to consider the internal resistance of the battery during the charging and discharging process is nonlinear changes^[3-5]. So this article selects Thevenin model for battery simulation^[6], and its equivalent model is shown in Figure 5.

In Figure 5: U_{oc} is the open circuit voltage; the ohmic internal resistance R_0 is determined by the internal structure of the battery and the electrolyte; the polarization internal resistance R_p is the resistance caused by the polarization effect when the battery positive and negative electrodes undergo a chemical reaction; C_p is the polarization capacitance. The parallel circuit of R_p and C_p describes the polarization process. According to the operating characteristics of the capacitor components, the relationship between the current flowing through the battery

polarization capacitor and its closed circuit voltage is obtained, as shown in formula (1).

$$I_p(t) = C_p \frac{dU_{Cp}(t)}{dt} \quad (1)$$

According to Kirchhoff's voltage law, the voltage relationship in the equivalent circuit can be obtained, as shown in formula (2).

$$R_o \times I_{Cp} + R_o \times \frac{U_{Cp}(t)}{R_p} + U_{Cp}(t) = U_{OC} - U_L \quad (2)$$

Combining formula (1) and formula (2), the state equation of the equivalent model is obtained, as shown in formula (3).

$$R_o \times C_p \frac{dU_{Cp}(t)}{dt} + \left(1 + \frac{R_o}{R_p}\right) U_{Cp}(t) = U_{OC} - U_L \quad (3)$$

The Thevenin equivalent model is suitable for a relatively stable state of SOC, which can better describe the dynamic and static performance of lithium batteries, and can accurately simulate the charging and discharging behavior of batteries under the conditions of current, temperature, and charge and discharge differences. At the same time, its structure is relatively simple, and it is widely used in dynamic modeling of power batteries. After parameter identification, modeling can be carried out. The parameter identification of 10Ah lithium battery is shown in Table 2, and the modeling is shown in Figure 6.

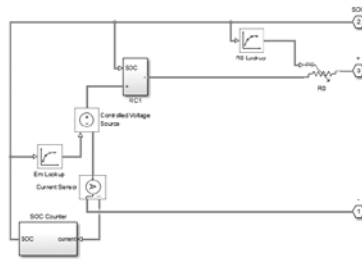


Figure 6: Thevenin battery model

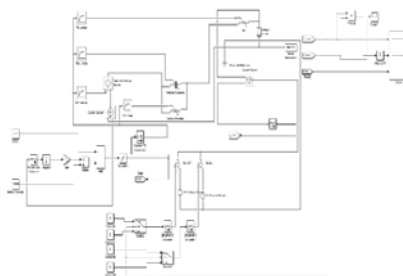


Figure 7: DC-DC constant current and constant voltage equivalent model

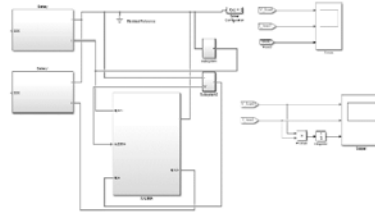


Figure 8: Equivalent model of the new scheme

Table 2: Parameter values

SOC	$R_0/m\Omega$	$R_p/m\Omega$	C_p/F	U_{oc}/V	SOC	$R_0/m\Omega$	$R_p/m\Omega$	C_p/F	U_{oc}/V
1.0	20.7	1.49	93317.1	3.40	0.5	19.6	1.21	47691.7	3.29
0.9	18.6	1.16	49748.1	3.34	0.4	20.3	1.59	36294.2	3.29
0.8	15.7	1.06	54440.5	3.32	0.3	23.4	1.67	34555.5	3.27
0.7	17.9	1.02	56575.4	3.30	0.2	24.9	1.46	39525.8	3.25
0.6	17.1	1.36	42431.6	3.30	0.1	28.6	1.59	22899.1	3.21

3.3 The comparison between the conventional and this article

The experiment is set to SOC to 95% to be full, and the model is to start when the battery is SOC 0.1. According to the scenario set above, the equivalent model of the constant voltage-constant current charging of the traditional common single battery is established as shown in Figure 7, and the equivalent model of the charging mode under the battery management method proposed in this article is shown in Figure 8.

Fig. 9 and Fig. 10 are the changes of the current and voltage with time and the battery SOC (State of charge) with time during the conventional constant current-constant voltage charging, respectively. From the image, at 30,000s, as the SOC rises, due to polarization, the image slope becomes smaller and smaller, and the battery charging speed will decrease. Figure 11 shows the changes of current and voltage with time under the dual-battery power management system and the comparison of the power of the two charging methods. The power management device switches when the SOC of the charged battery reaches 0.8, and starts charging another battery. From the image, the charging characteristics of the battery to the individual battery through the management device are basically the same. But the new scheme switched to another battery when the charging power dropped, and the power increased.

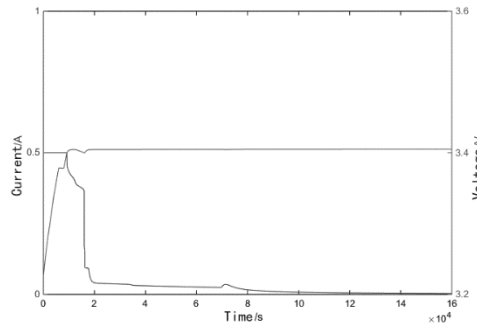


Figure 9 Battery current and voltage changes under constant current and constant voltage

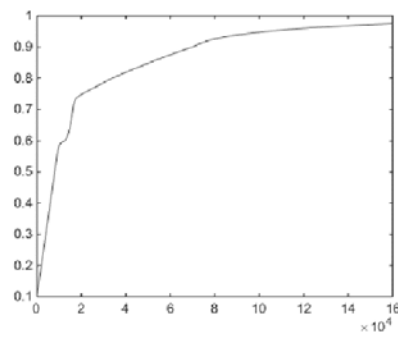


Figure 10: Battery SOC change under constant current and constant voltage

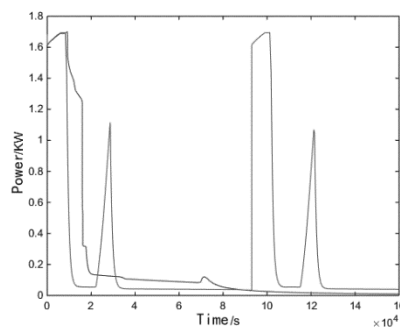


Figure 11 Comparison of charging power

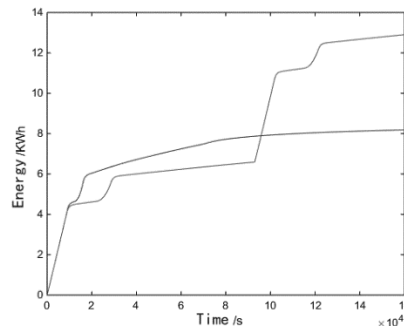


Figure 12 Charging energy comparison

In the use scenario as a solar battery, a relatively high charging efficiency should be ensured to ensure the stability of energy supply. Fig. 12 is a comparison between the battery charging condition in the normal constant voltage-constant current charging mode and the battery charging condition in the case of dual power management.

It is simulated that when the time reaches 160000s, the energy collected by the traditional scheme is 8.23KWh. The design scheme in this paper collects 12.9KWh of energy. 56% improvement over traditional methods.

4. Conclusions

Compared with the traditional power supply system, the battery management system designed in this paper further improves the charging efficiency of using solar energy for charging in farmland application scenarios. The relative reduction of the solar panel area can also achieve the same effect as before, greatly facilitating agricultural products the miniaturization of the design of networked products, and the overcharge and overdischarge protection of the battery further improve the stability of the product.

References

- [1] Qiu Yingying. Analysis of the application solutions for the power system of agricultural Internet of Things [J]. Guangxi Agricultural Science, 2016, 31 (6): 61-64. DOI: 10.3969 / j.issn.1003-4374.2016.06.018.
- [2] Wang Jufen, Yang Haiping, Li Xuanfu. Design of battery overcharge and discharge control system in photovoltaic system [J]. Battery Industry, 2003, 8 (6): 275-277. DOI: 10.3969 / j.issn.10087-923.2003. 06.009.
- [3] Li Baihua, Guo Canbin, Zhong Qishui. Research on parameter identification of the Thevenin equivalent circuit model of lithium batteries for electric vehicles [J].

- Microcomputer and Application, 2017, 36 (1): 83-85, 88. DOI: 10.19358 / j.issn.1674-7720.2017.01.025.
- [4] Chen Yuanli, Zhao Zhendong, Chen Sujuan. Simulink-based ternary lithium battery modeling and simulation research [J]. Journal of Nanjing Institute of Technology (Natural Science Edition) 2019, 17 (3): 1620. DOI: 10.13960 / j.issn.1672-2558.2019.03.003.
- [5] Li Baihua, Guo Canbin, Zhong Qishui, et al. Parameter identification of the Thevenin equivalent circuit model of lithium batteries for electric vehicles [J]. Microcomputers and Applications, 2017, 36 (1): 83-85, 88. DOI: 10.19358 / j.issn.1674-7720.2017.01.025.
- [6] Wang Chenyi, Wang Shunli, Chen Yixin, et al. Analysis and characterization of the working characteristics of lithium iron phosphate batteries for pure electric vehicles [J]. Automation Instrumentation, 2019, 40 (8): 13-17. DOI: 10.16086 / j.cnki.issn1000-0380.2018100001.